Bull. Korean Chem. Soc. **2014**, Vol. 35, No. 5 1511
http://dx.doi.org/10.5012/bkcs.2014.35.5.1511

CASPT2 Study on the Low-lying Electronic States of 1,3,5-$C_6H_3Cl_3^+$ Ion

Shu-Yuan Yu,[†,*] Cheng-Gen Zhang,[†,‡] and Shu-Jun Wang[†]

[†]*Department of Chemistry and Material Science, Langfang Normal College, Langfang 065000, People's Republic of China*
[*]*E-mail: yushuyuan05@mails.ucas.ac.cn*
[‡]*College of Chemistry and Chemical Engineering, University of Chinese Academy of Sciences, Beijing 100049, People's Republic of China*
Received October 13, 2013, Accepted January 30, 2014

The multiconfiguration second-order perturbation theory (CASPT2) and complete active space self-consistent field (CASSCF) methods were employed to calculate the geometries and energy levels for the low-lying electronic states of 1,3,5-$C_6H_3Cl_3^+$ ion. The CASPT2 values for the 1,3,5-$C_6H_3Cl_3^+$ ion were in reasonable agreement with the available experimental values. The current calculations augmented previous theoretical investigations on the ground state and assigned the low-lying excited electronic states of the 1,3,5-$C_6H_3Cl_3^+$ ion. The Jahn-Teller distortion in the excited electronic state for the 1,3,5-$C_6H_3Cl_3^+$ ion were reported for the first time.

Key Words : CASPT2, Electronic states, Excitation energies, Jahn-Teller effect, Geometries

Introduction

Halobenzene ions have long attracted a great deal of interest for its great significance for environmental protection.[1,2] The 1,3,5-$C_6H_3Cl_3^+$ ion has been investigated by spectroscopic studies.[3-8] The experimental adiabatic ionization potential (AIP) values and vertical ionization potential (VIP) values for the 1,3,5-$C_6H_3Cl_3^+$ ion were reported by Maier *et al.*.[3] Assignments of electronic states are fundamental to understanding of the experimental facts. On the basis of the energy orderings of the four highest-occupied molecular orbitals (HOMOs) in the electronic configurations of the ground-state 1,3,5-$C_6H_3Cl_3$ ($\ldots 12e'^4\ 3a_2'^2\ 3a_2''^2\ 3e''^4$) molecule, the four lowest-lying states of the 1,3,5-$C_6H_3Cl_3^+$ ion could be assigned to X^2E'', A^2A_2'', B^2A_2' and C^2E', respectively. One of the main topics of interest in the spectroscopic investigation of highly symmetric cations such as 1,3,5-$C_6H_3Cl_3^+$ is the Jahn-Teller effect because of the degenerate $^2E''$ and $^2E'$ states. The Jahn-Teller effect splits the degenerate electronic states involved in D_{3h} symmetry ($^2E''$ and $^2E'$) to corresponding electronic states in low (such as C_{2v}) symmetry. So those four electronic states mentioned above for the 1,3,5-$C_6H_3Cl_3^+$ ion were assigned to X^2E'', B^2A_2'', C^2A_2', and D^2E', respectively, in which the X^2E'' and D^2E' states correspond to the points of the conical intersection of the Jahn-Teller potential energy surfaces (PESs).

The Jahn-Teller effect for the 1,3,5-$C_6H_3Cl_3^+$ ion in the ground electronic state has been investigated by mass-analyzed threshold ionization (MATI) spectroscopy[4] and wavelength resolved emission spectra.[5] Most of these focus on the Jahn-Teller active vibrational mode of the ground electronic state and the Jahn-Teller stabilization energy of the ground state.

Theoretical studies of the 1,3,5-$C_6H_3Cl_3^+$ ion have been few. The ground state of the 1,3,5-$C_6H_3Cl_3^+$ ion were previously calculated by using the DFT[9] and GRHF[10] methods. In the literature we have found no reported theoretical studies on excited electronic states of 1,3,5-$C_6H_3Cl_3^+$ ion, and there are neither experimental nor theoretical studies on the Jahn-Teller distortion in the higher electronic state ($^2E'$) for the 1,3,5-$C_6H_3Cl_3^+$ ion reported. The molecular configurations distortion owing to the Jahn-Teller effect and the corresponding electronic states in low symmetry are of particular interest herein.

It is known that the CASSCF (complete active space self-consistent field)[11] and CASPT2 (multiconfiguration second-order perturbation theory) methods[12,13] are effective for theoretical studies of excited electronic states of molecules and molecular ions.[14-17] In the present work the six lowest-lying electronic states of the 1,3,5-$C_6H_3Cl_3^+$ ion were studied using the CASPT2 and CASSCF methods. The Jahn-Teller distortion in the X^2E'' and D^2E' states, equilibrium geometries and excitation energies of the states were calculated. These results are described and discussed below, and the assignments for the *X*, *A*, *B*, *C*, *D*, and *E* states of 1,3,5-$C_6H_3Cl_3^+$ ion based on our CASPT2 calculations are presented. Only the 1,3,5-isomers of the $C_6H_3Cl_3^+$ ion were involved. So the "1,3,5-" designation will be omitted from hereon.

Calculation Details

The CAS (CASSCF and CASPT2) calculations were carried out using the MOLCAS 7.8 quantum-chemistry software.[18] With a CASSCF wavefunction constituting the reference function, the CASPT2 calculations were performed to compute the first-order wavefunction and the second-order energy in the full-CI space. A contracted atomic natural orbital (ANO-L) basis set,[19-21] Cl[5s4p2d1f]/F[4s3p2d]/C[4s3p2d]/H[3s2p1d], was used. It was assumed that the electronic states of the $C_6H_3Cl_3^+$ ion studied in the present

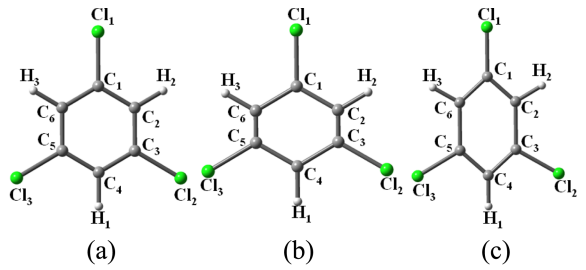

Figure 1. Atom labelings for the $C_6H_3Cl_3^+$ ion used in the present work, (a) in D_{3h} symmetry, (b) and (c) in C_{2v} symmetry resulting from the Jahn-Teller distortion.

work have planar geometries in D_{3h} symmetry and in C_{2v} symmetry (resulting from the Jahn-Teller distortion), and the geometries and atom labels used for the $C_6H_3Cl_3^+$ ion are shown in Figure 1(a), (b), and (c).

The CASPT2 and CASSCF geometry optimization calculations were performed for the electronic states of the $C_6H_3Cl_3^+$ ion, and the CASSCF frequency calculations were performed for all the calculated C_{2v} and D_{3h} states. On the basis of the CASPT2 energies of the X^2B_1 ground state (see below) and the excited states calculated at the respective CASPT2 and CASSCF optimized geometries of the $C_6H_3Cl_3^+$ ion, we obtained the CASPT2//CASPT2 and CASPT2//CASSCF adiabatic excitation energy values (denoted as CASPT2 T_0 and CASPT2//CASSCF T_0, respectively) for the excited states. On the basis of the CASPT2 energies of the X^2B_1 and excited states calculated at the CASPT2 geometry of the X^2B_1 ground state of the $C_6H_3Cl_3^+$ ion, we obtained the CASPT2 vertical excitation energy values (denoted as CASPT2 T_v) for the excited states. On the basis of the CASPT2 energies of the X^2B_1 and excited states calculated at the experimental ground-state geometry of 1,3,5-$C_6H_3Cl_3$ molecules,[6] we obtained the CASPT2 relative energy values (denoted as CASPT2 T_v') for the electronic states of the $C_6H_3Cl_3^+$ ion.

In the CAS calculations for the low-lying states of the $C_6H_3Cl_3^+$ ion, 11 electrons were active and the active space included 12 orbitals [CAS (11,12)]. The choice of active space stemmed from the molecular orbital (MO) sequence of the ground-state 1,3,5-$C_6H_3Cl_3$ molecule. The highest symmetry point-group is D_{2h} for the CASSCF wavefunction in MOLCAS software, so the C_{2v} point-group, the sub-group of D_{3h}, was used in the present work. Based on the HF/6-31+G(d,p) calculations, the ground-state 1,3,5-$C_6H_3Cl_3$ molecule has the following electron configuration: $\ldots(4b_1)^2(2a_2)^2(14b_2)^2(21a_1)^2(15b_2)^2(5b_1)^2(3a_2)^2(6b_1)^2(22a_1)^0(23a_1)^0(16b_2)^0(4a_2)^0(7b_1)^0(17b_2)^0(24a_1)^0(25a_1)^0(8b_1)^0\ldots$. Our active space corresponded to a segment of this sequence from $14b_2$ to $7b_1$, augmented with $8b_1$ for $C_6H_3Cl_3^+$. The selected active space is composed of six π/π^* orbitals of the phenyl ring, two σ/σ^* orbitals of C–Cl, two p orbitals of Cl_1, and two p orbitals of Cl_2 and Cl_3. Labeling these orbitals (six occupied plus six virtual) within the C_{2v} point-group in the order a_1, a_2, b_2, and b_1, this active space was named (3234). In CAS calculations for electronic states of a molecular ion, we often take a "segment" of the electron configuration of the ground-state molecule constituting our active space. The "segment" includes many (sequential) occupied MOs for not missing primary ionization states and includes a few of virtual MOs for describing shake-up ionization character of some ionic states. And this way of the choice of the active space has been justified by our previous published works on electronic states of halobenzene ions,[15-17] in which the CASPT2 calculations predict more accurate results for the electronic states of these ions. At the same time, the testing CASPT2 T_v' calculations for the $C_6H_3Cl_3^+$ ion using larger active spaces, CAS(15,12) and CAS(15,14) were performed [Details are given in the supporting information (SI1)] and

Table 1. CASPT2 and CASSCF optimized geometries[a] for the $1^1A_1'$ (X^1A_1') state of the 1,3,5-$C_6H_3Cl_3$ molecule and for the 1^2B_1, 1^2A_2, $1^2A_2''$, $1^2A_2'$, 2^2B_2, and 1^2A_1 states of the $C_6H_3Cl_3^+$ ion (bond lengths are given in Å and bond angles in degrees; for atom labelings, see Figure 1)

State	Method	$R(C_1\text{-}Cl_1)$	$R(C_3\text{-}Cl_2)$	$R(C_1\text{-}C_2)$	$R(C_2\text{-}C_3)$	$R(C_3\text{-}C_4)$	$\angle C_2C_1C_6$	$\angle C_1C_2C_3$	$\angle C_3C_4C_5$
$1^1A_1'$	CASPT2	1.725		1.391			121.9		118.0
	CASSCF	1.735		1.391			121.8		118.2
	Exptl.[b]	1.728		1.394			122.4		117.6
1^2B_1	CASPT2	1.662	1.691	1.422	1.374	1.424	122.8	118.2	120.9
	CASSCF	1.677	1.703	1.421	1.386	1.427	122.8	118.3	121.0
1^2A_2	CASPT2	1.700	1.672	1.391	1.442	1.388	119.1	119.9	117.4
	CASSCF	1.710	1.687	1.406	1.440	1.386	118.9	119.7	118.2
$1^2A_2''$	CASPT2	1.677		1.411			122.0		118.0
	CASSCF	1.686		1.428			121.2		118.8
$1^2A_2'$	CASPT2	1.702		1.398			123.2		116.8
	CASSCF	1.720		1.397			122.9		117.1
2^2B_2	CASPT2	1.734	1.713	1.394	1.382	1.404	121.7	117.6	114.4
	CASSCF	1.745	1.728	1.399	1.381	1.400	120.9	118.8	113.3
1^2A_1	CASPT2	1.709	1.728	1.393	1.397	1.387	122.4	117.0	115.8
	CASSCF	1.716	1.748	1.392	1.390	1.383	121.7	117.4	115.9

[a]Only geometric parameters in the heavy-atom frame-works are given. [b]The experimental geometry of the ground-state 1,3,5-$C_6H_3Cl_3$ molecule, see Ref. 6.

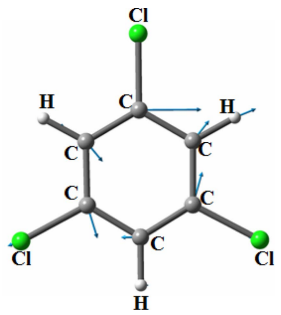

Figure 2. The vibrational mode for the imaginary frequency.

the calculated T_v' values are similar to the CASPT2 T_v' values obtained in the CAS(11,12) calculations. In all the CASPT2 calculations the weight values of the CASSCF reference functions in the first-order wave functions were larger than 0.75.

Results and Discussion

Optimized Geometries. As a non-linear polyatomic system, the $C_6H_3Cl_3^+$ ion (D_{3h}) in the degenerate X^2E'' and D^2E' states should experience the Jahn-Teller geometry distortion and reduce the symmetry from D_{3h} to C_{2v}. The X^2E'' state splits into one $^2B_1$ state and one $^2A_2$ state at two different C_{2v} geometries, and the D^2E' state splits into one $^2A_1$ state and one $^2B_2$ state at two different C_{2v} geometries.

In Table 1, the CASPT2 and CASSCF optimized geometries for the 1^2B_1, 1^2A_2, $1^2A_2''$, $1^2A_2'$, 2^2B_2, and 1^2A_1 states of the $C_6H_3Cl_3^+$ ion are given, together with the CASPT2 and CASSCF optimized geometries and experimental geometry[6] for the $1^1A_1'$ ground state of the 1,3,5-$C_6H_3Cl_3$ molecule. The CASSCF frequency calculations produced no imaginary frequencies for the 1^2B_1, $1^2A_2''$, $1^2A_2'$, and 2^2B_2 states, indicating that the CASSCF geometries of the four states correspond to energy minima in the respective PESs, and thus the CASPT2 and CASSCF optimized geometries were considered to be the predicted equilibrium geometries. The CASSCF frequency calculations for the 1^2A_2 and 1^2A_1 states produced the unique imaginary frequency of the b_2 symmetry and represent saddle points. The vibrational modes for the imaginary frequencies of the 1^2A_2 and 1^2A_1 states are similar, they principally involving the C-C-C bending in the phenyl ring that likely reduces the molecular symmetry from D_{3h} to C_{2v}. This is consistent with the conclusions of the previous experiment[5,8] that the C-C-C bending mode is the most active Jahn-Teller mode in $C_6H_3Cl_3^+$ ion. And the vibrational mode for the imaginary frequency is shown schematically in Figure 2.

The CASPT2 optimized geometry for the $1^1A_1'$ ground state of the 1,3,5-$C_6H_3Cl_3$ molecule was almost identical to the experimental geometry,[6] while the C-Cl bond length values in the CASSCF optimized geometries were 0.007 Å larger than the experimental value, respectively. For the ionic states of the $C_6H_3Cl_3^+$ ion (1^2B_1, 1^2A_2, $1^2A_2''$, $1^2A_2'$, 2^2B_2, and 1^2A_1), the CASSCF calculations predicted longer C-Cl bond lengths than the CASPT2 calculations. The CASPT2 calculations predicted more accurate geometries for the ground-state halobenzene molecules than the CASSCF calculations based on our previous studies.[15-17] It was expected that the CASPT2 calculations would predict accurate geometries for the ground and excited states of the $C_6H_3Cl_3^+$ ion.

As shown in Table 1, the CASPT2 geometries for the 2^2B_2 and 1^2A_1 states (the two Jahn-Teller component states of D^2E') are noticeably different. The C_1-Cl_1 bond length is longer than the C_3-Cl_2 bond length in the 2^2B_2 state while the C_1-Cl_1 bond length is shorter than the C_3-Cl_2 bond length in the 1^2A_1 state, and the differences of the two C-Cl bond lengths are almost equal for the two states. The C_1-C_2 and C_3-C_4 bond lengths are longer than the C_2-C_3 bond length (0.012 and 0.022 Å, respectively) in the 2^2B_2 state, while the C_1-C_2 and C_3-C_4 bond lengths are shorter than the C_2-C_3 bond length (0.004 and 0.010 Å, respectively) in the 1^2A_1 state. This signifies that the carbon frameworks of the CASPT2 geometries (C_{2v}) for the two states (2^2B_2 and 1^2A_1) are regular hexagons distorted to significant extents because of the Jahn-Teller effect, and that one of the carbon frames is "flattened" and the other is "elongated" [see Figure 1(b) and (c)]. The CASPT2 geometries for the 1^2B_1 and 1^2A_2 states (the two Jahn-Teller component states of X^2E'') are also notably different. The carbon frameworks of the CASPT2 geometries (C_{2v}) for the two states (1^2B_1 and 1^2A_2) are regular hexagons distorted to great extents because of the Jahn-Teller effect, and one of the carbon frames is "flattened" and the other is "elongated" [see Figure 1(b) and (c)].

Excitation Energies. In Table 2 the CASPT2 and CASPT2//CASSCF T_0 values for the 1^2B_1, 1^2A_2, $1^2A_2''$, $1^2A_2'$, 2^2B_2, and 1^2A_1 states of the $C_6H_3Cl_3^+$ ion are given, along with the CASPT2 T_v and T_v' values for the six states. The experimental T_0 value for the B state and the experimental T_v' values for the B, C, and D states are also listed in Table 2.

By checking the CASSCF wavefunctions, the 1^2B_1, 1^2A_2, $1^2A_2'$ (1^2B_2 in C_{2v} symmetry), 2^2B_2, and 1^2A_1 states could be characterized as primary ionized states. Our CASPT2 and

Table 2. Calculated energetic results (in eV) for the 1^2B_1, 1^2A_2, $1^2A_2''$, $1^2A_2'$, 2^2B_2, and 1^2A_1 states of the $C_6H_3Cl_3^+$ ion: CASPT2 and CASPT2//CASSCF adiabatic excitation energy (T_0) values, CASPT2 vertical excitation energy (T_v) values, and CASPT2 relative energy (T_v') values calculated at the experimental ground-state geometry of the 1,3,5-$C_6H_3Cl_3$ molecule[a]

State	T_0			T_v	T_v'	
	CASPT2	CASPT2 //CASSCF	Exptl.[b]	CASPT2	CASPT2	Exptl.[b]
1^2B_1	0.0	0.0	0.0 (X)	0.0	0.0	0.0 (X)
1^2A_2	0.014	0.019		0.40	0.016	
$1^2A_2''$	1.98	1.94	1.91 (B)	2.07	1.90	1.91 (B)
$1^2A_2'$	2.03	2.00		2.17	2.09	2.17 (C)
2^2B_2	2.28	2.24		2.35	2.30	2.59 (D)
1^2A_1	2.36	2.33		2.48	2.43	

[a]The experimental geometry of the ground-state 1,3,5-$C_6H_3Cl_3$ molecule, see Ref. 6. [b]Ref. 3

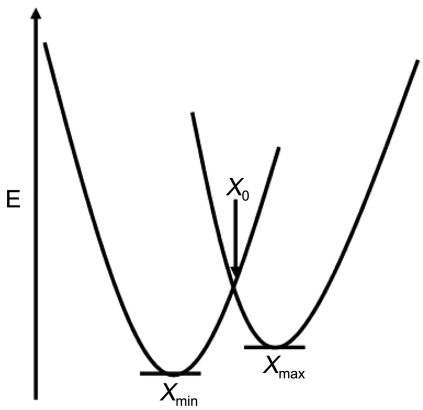

Figure 3. A slice through the Jahn-Teller potential energy surface.

CASPT2//CASSCF T_0 calculations indicated that 1^2B_1 is the ground state of the $C_6H_3Cl_3^+$ ion. On the basis of our CASPT2 T_0 values the *X*, *A*, *B*, *C*, *D*, and *E* states of the $C_6H_3Cl_3^+$ ion were assigned to the 1^2B_1, 1^2A_2, $1^2A_2''$, $1^2A_2'$, 2^2B_2, and 1^2A_1 states, respectively. The CASPT2 T_0 value of 1.98 eV for the $1^2A_2''$ state was in good agreement with the experimental T_0 value of 1.91 eV for the *B* state.[3] The CASPT2//CASSCF T_0 values for the six states were similar to the CASPT2 T_0 values for the respective states.

Based on our CASPT2 T_0 results the 1^2A_2 state is higher in energy than the 1^2B_1 state by 0.014 eV. As described above, the geometries of the 1^2B_1 and 1^2A_2 states (the two Jahn-Teller component states of X^2E'') are regular hexagons distorted into "flattened" and "elongated" [see Figure 1(b) and (c)] carbon frames, respectively, and the CASSCF frequency calculations produced no imaginary frequency for the 1^2B_1 state and one imaginary frequency for the 1^2A_2 state. These facts indicate that the symmetry distortion of $C_6H_3Cl_3^+$ from D_{3h} to C_{2v} by the Jahn-Teller effect splits the ground electronic state X^2E'' into 1^2B_1 and 1^2A_2 states, and 1^2B_1 (C_{2v}), 1^2A_2 (C_{2v}), and X^2E'' (D_{3h}) correspond to the global minimum (X_{min}), the saddle point (X_{max}), and the conical intersection (X_0) on the PES, respectively, as shown in Figure 3. The relative energy of the X_0 and X_{min} ($E_{X_0} - E_{X_{min}}$) is generally accepted as the total Jahn-Teller stabilization energy. The CASPT2 value of Jahn-Teller stabilization energy for the ground state is 0.090 eV, which is in reasonable agreement with the experimental value of 547 cm^{-1} (0.068 eV).[8]

The CASPT2 T_0 value for the 1^2A_1 state is larger than that for the 2^2B_2 state by 0.08 eV. As described above, the geometries of the 2^2B_2 and 1^2A_1 states (the two Jahn-Teller component states of D^2E') are also "flattened" and "elongated" distortions of regular hexagonal [see Figure 1(b) and (c)] carbon frames, respectively, and the CASSCF frequency calculations produced no imaginary frequency for the 2^2B_2 state and one imaginary frequency for the 1^2A_1 state. These facts indicate that the symmetry distortion of $C_6H_3Cl_3^+$ from D_{3h} to C_{2v} by the Jahn-Teller effect splits the excited electronic state D^2E' into 2^2B_2 and 1^2A_1 states, and 2^2B_2 (C_{2v}), 1^2A_1 (C_{2v}), and D^2E' (D_{3h}) correspond to the global minimum (X_{min}), the saddle point (X_{max}), and the conical intersection (X_0) on the PES, respectively, as shown in Figure 3. The CASPT2 value of Jahn-Teller stabilization energy for the excited state is 0.151 eV.

As shown in Table 2, the CASPT2 T_v and T_v' orderings for the 1^2B_1, 1^2A_2, $1^2A_2''$, $1^2A_2'$, 2^2B_2, and 1^2A_1 states are the same as the CASPT2 T_0 ordering. The CASPT2 T_v' values of 1.90 and 2.09 eV for the $1^2A_2''$ and $1^2A_2'$ states are in good agreement with the experimental T_v' values of 1.91 and 2.17 eV for the *B* and *C* states evaluated using the experimental VIP values, respectively (the deviations being smaller than 0.08 eV).[3]

Conclusion

Geometries and energy levels for the low-lying electronic states of the $C_6H_3Cl_3^+$ ion were calculated by using the CASPT2 and CASSCF methods in conjunction with the ANO-L basis set. The CASPT2 values for the $C_6H_3Cl_3^+$ ion were in reasonable agreement with the available experimental values. Based on our CASPT2 and CASSCF T_0 calculations, we assigned the *X*, *A*, *B*, *C*, *D*, and *E* states of $C_6H_3Cl_3^+$ to 1^2B_1, 1^2A_2, $1^2A_2''$, $1^2A_2'$, 2^2B_2, and 1^2A_1, respectively.

The Jahn-Teller distortion in the excited electronic state for the $C_6H_3Cl_3^+$ ion were reported for the first time. The symmetry distortion of $C_6H_3Cl_3^+$ from D_{3h} to C_{2v} by the Jahn-Teller effect split the ground state X^2E'' into 1^2B_1 and 1^2A_2 states and split the excited state D^2E' into 2^2B_2 and 1^2A_1 states. The carbon frameworks of the CASPT2 geometries for the two Jahn-Teller component states of $C_6H_3Cl_3^+$ ion were regular hexagons distorted to be "elongated" or "flattened " carbon frames, respectively, because of the Jahn-Teller effect.

Acknowledgments. We express our thanks for financial support from the National Science Foundation of China (Nos. 21303078 and 21373217), the Hebei Province Science Foundation for Youths (B2012408008) and the Educational Commission of Hebei Province (Y2012023).

References

1. Molski, M. J.; Mollenhauer, D.; Gohr, S.; Paulus, B.; Khanfar, M. A.; Shorafa, H.; Strauss, S. H.; Seppelt, K. *Chem. Eur. J.* **2013**, *18*, 6644.
2. Cleland, D.; McCluskey, A. *Org. Biomol. Chem.* **2013**, *11*, 4672.
3. Maier, J. P.; Marthaler, O. *Chem. Phys.* **1978**, *32*, 419.
4. Witte, F.; Riese, M.; Gunzer, F.; Grotemeyer, J. *Int. J. Mass Spectrom.* **2011**, *306*, 129.
5. Sears, T.; Miller, T. A.; Bondybey, V. E. *J. Chem. Phys.* **1980**, *72*, 6749.
6. Blom, R.; Cradock, S.; Davidson, S. L.; Rankin, D. W. H. *J. Mol. Struct.* **1991**, *245*, 369.
7. Schlag, E. W. *ZEKE Spectroscopy*; Cambridge University Press: Cambridge, 1998.
8. Sears, T.; Miller, T. A.; Bondybey, V. E. *J. Chem. Phys.* **1980**, *72*, 6070.
9. Cheng, J.-B.; Liu, H. C.; Li, W.-Z.; Li, Q. Z.; Yu, J. K.; Gong, B. A.; Sun, C. C. *Chem. J. Chinese U* **2010**, *31*, 1446.

10. Applegate, B. E.; Miller, T. A. *J. Chem. Phys.* **2002**, *117*, 10654.
11. Roos, B. O. In *Ab Initio Methods in Quantum Chemistry*; Lawley, K. P., Ed.; Part 2, Wiley: New York, 1987; pp 399-446.
12. Andersson, K.; Malmqvist, P. A.; Roos, B. O.; Sadley, A. J.; Wolinski, K. *J. Phys. Chem.* **1990**, *94*, 5483.
13. Andersson, K.; Malmqvist, P. A.; Roos, B. O. *J. Chem. Phys.* **1992**, *96*, 1218.
14. Li, W.-Z.; Chen, S.-F.; Liu, Y.-J. *J. Chem. Phys.* **2011**, *134*, 114303.
15. Yu, S.-Y.; Huang, M.-B. *Chem. Phys.* **2006**, *328*, 291.
16. Yu, S.-Y.; Huang, M.-B. *J. Mol. Struct.: THEOCHEM* **2007**, *822*, 48.
17. Yu, S.-Y.; Zhang, C.-G. *J. Mol. Spectrosc.* **2014**, *295*, 58.
18. Andersson, K.; Aquilante, F.; Barysz, M.; Bernhardsson, A.; Blomberg, M. R. A.; Carissan, Y.; Cooper, D. L.; Cossi, M.; DeVico, L.; Ferré, N.; Fülscher, M. P.; Gaenko, A.; Gagliardi, L.; Ghigo, G.; Graaf, C.; Gusarov, S.; Hess, B. A.; Hagberg, D.; Holt, A.; Karlström, G.; Lindh, R.; Malmqvist, P.-Å.; Nakajima, T.; Neogrády, P.; Olsen, J.; Pedersen, T.; Pitonak, M.; Raab, J.; Reiher, M.; Roos, B. O.; Ryde, U.; Schimmelpfennig, B.; Schütz, M.; Seijo, L.; Serrano-Andrés, L.; Siegbahn, P. E. M.; Stålring, J.; Thorsteinsson, T.; Veryazov, V.; Widmark, P.-O. MOLCAS (version 7.8), University of Lund, Sweden, 2012.
19. Almlof, J.; Taylor, P. R. *J. Chem. Phys.* **1987**, *86*, 4070.
20. Widmark, P. O.; Malmqvist, P. A.; Roos, B. O. *Theor. Chim. Acta* **1990**, *77*, 291.
21. Widmark, P. O.; Persson, B. J.; Roos, B. O. *Theor. Chim. Acta* **1991**, *79*, 419.